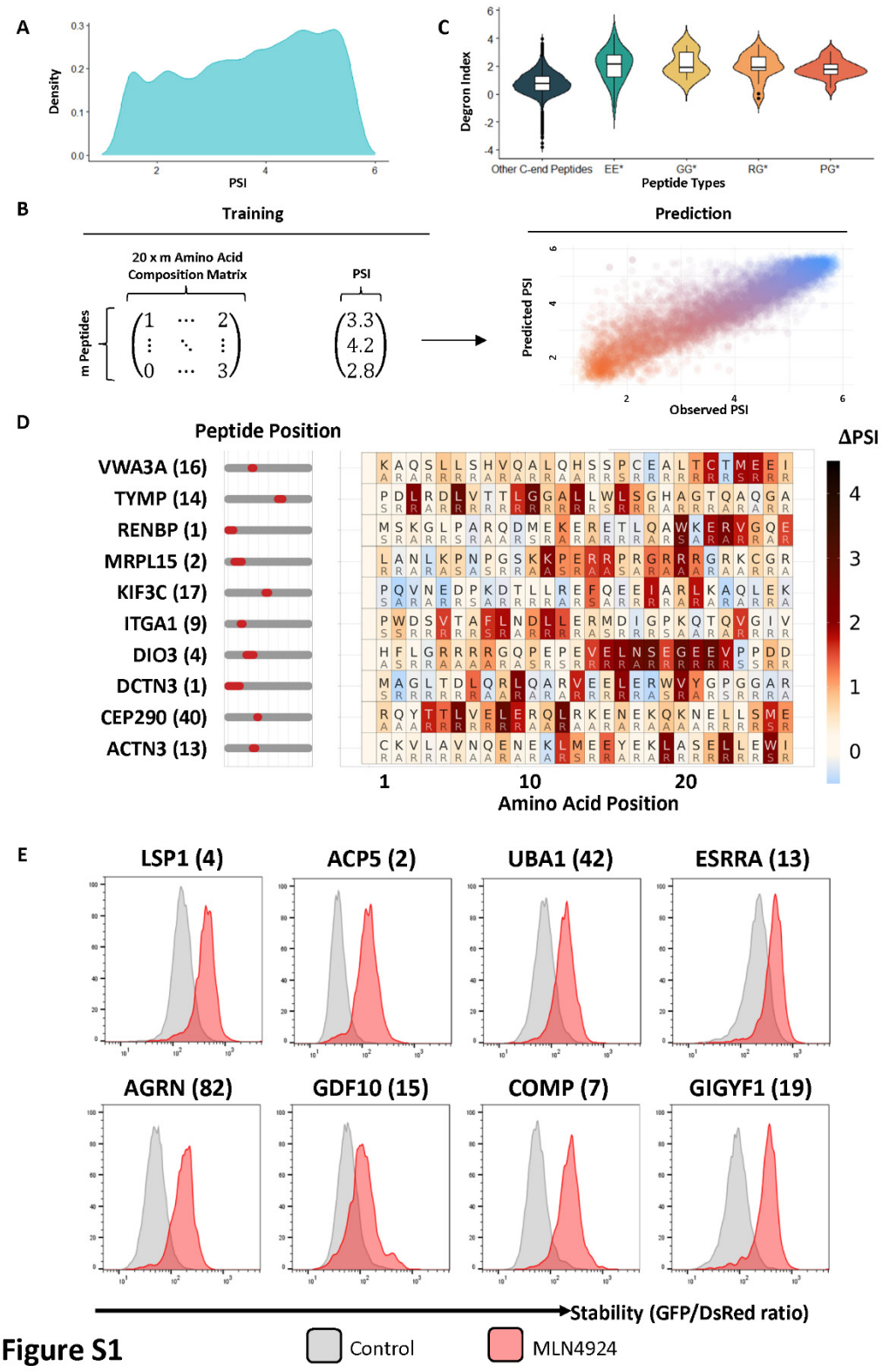
A
Density
PSI
C
Degron Index
Other C-end Peptides
EE*
GG*
RG*
PG*
Peptide Types
B
Training
20 x m Amino Acid Composition Matrix
m Peptides
PSI
Prediction
Predicted PSI
Observed PSI
D
Peptide Position
VWA3A (16)
TYMP (14)
RENBP (1)
MRPL15 (2)
KIF3C (17)
ITGA1 (9)
DIO3 (4)
DCTN3 (1)
CEP290 (40)
ACTN3 (13)
Amino Acid Position
ΔPSI
E
LSP1 (4)
ACP5 (2)
UBA1 (42)
ESRRA (13)
AGRN (82)
GDF10 (15)
COMP (7)
GIGYF1 (19)
Stability (GFP/DsRed ratio)
Control
MLN4924

Figure S1

Figure S1. GPS-peptidome screen identified many unstable peptides. Related to Figure 1, Figure 2, and Figure 3.

(A) Distribution of the PSI of individual peptides.

(B) Schematic diagram illustrating the workflow of SVM machine learning. Correlations between the experimentally observed PSIs and machine learning predict the PSI of each peptide is shown for 10K randomly selected peptides which are depicted as dots. Dots above the diagonal deviate from the predicted PSI and are candidates that may contain degrons.

(C) Population of peptides containing known degrons[14] (EE*, GG*, RG*, PG*) have significantly larger degron indexes than the distribution of the other C-end peptides from the 28-mer peptidome library. Degron index = Predicted PSI – Observed PSI.

(D) Scanning mutagenesis of representative non-CRL degron peptides with diverse degron motifs. The darker the color, the larger the degree of stabilization by the corresponding mutation

(E) Eight representative peptides identified as responsive to MLN4924 were individually examined by treatment with 1 uM MLN4924 for 24 h to assay stability as denoted by the GFP/DsRed ratio.

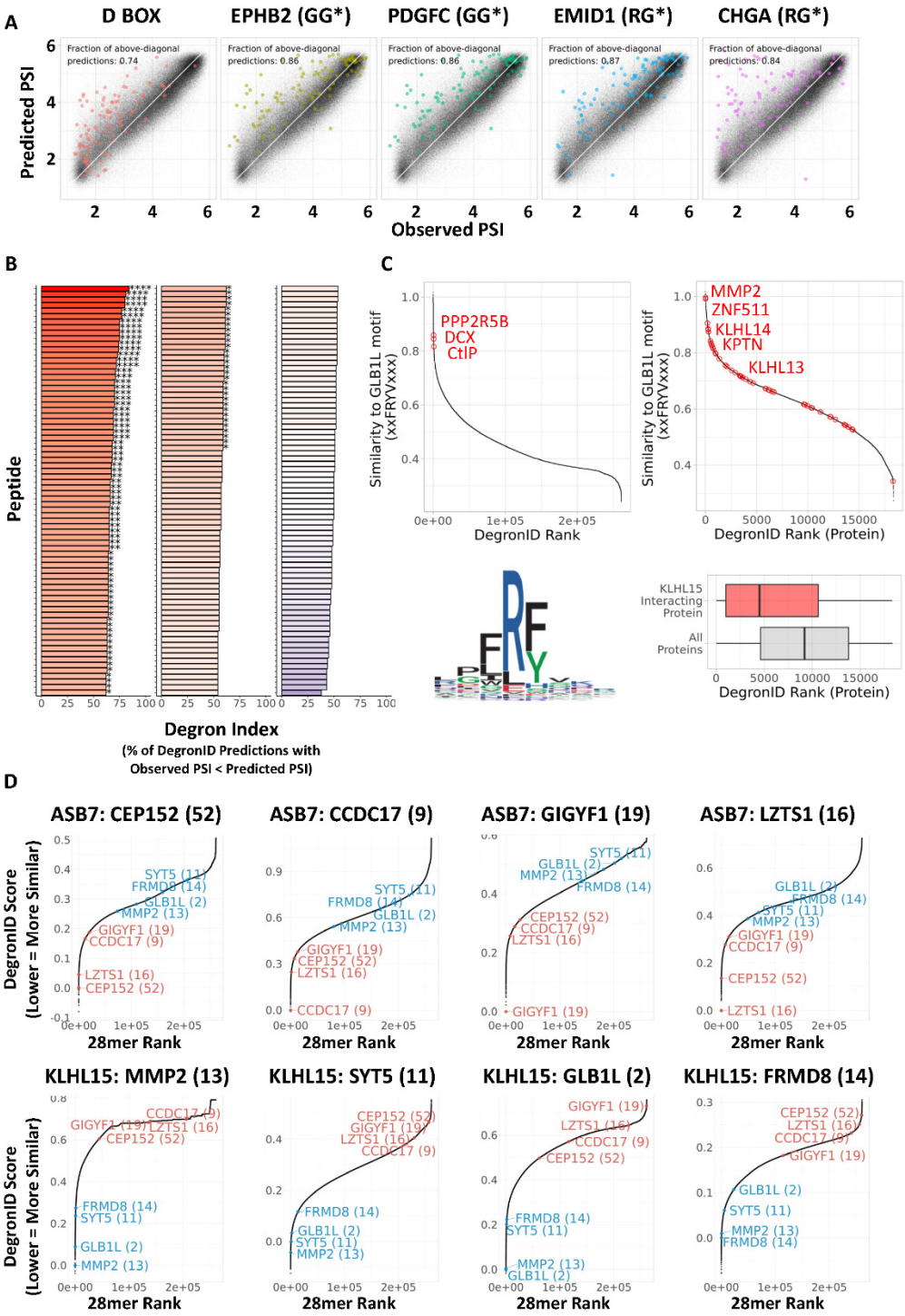
A
D BOX
EPHB2 (GG*)
PDGFC (GG*)
EMID1 (RG*)
CHGA (RG*)
Fraction of above-diagonal predictions: 0.74
Fraction of above-diagonal predictions: 0.86
Fraction of above-diagonal predictions: 0.86
Fraction of above-diagonal predictions: 0.87
Fraction of above-diagonal predictions: 0.84
Predicted PSI
Observed PSI
B
Peptide
Degron Index
(% of DegronID Predictions with Observed PSI < Predicted PSI)
C
PPP2R5B
DCX
CtIP
Similarity to GLB1L motif (xxFRYVxxx)
DegronID Rank
MMP2
ZNF511
KLHL14
KPTN
KLHL13
DegronID Rank (Protein)
KLHL15 Interacting Protein
All Proteins
D
ASB7: CEP152 (52)
ASB7: CCDC17 (9)
ASB7: GIGYF1 (19)
ASB7: LZTS1 (16)
KLHL15: MMP2 (13)
KLHL15: SYT5 (11)
KLHL15: GLB1L (2)
KLHL15: FRMD8 (14)
DegronID Score (Lower = More Similar)
28mer Rank

Figure S2

Figure S2. Degron ID classified saturation mutagenesis motifs into clusters based on their sequence similarities. Related to Figure 4.

(A) Benchmarking of the DegronID method. For D-box degrons from APC/C, along with saturation mutagenesis heatmaps from previously characterized C-terminal degrons the DegronID algorithm was performed and the 200 peptides that most closely resemble the starting motif are colored.

(B) 219 individual degron prediction models sorted by percentage of the top 200 predicted hits from each degron prediction model that are less stable than expected based on amino acid composition. Asterisks indicate FDR significance level (**** FDR < 0.0001, *** FDR < 0.001, ** FDR < 0.01, * FDR < 0.1). Significance calculated relative to a null distribution defined by repeated random sampling of 100 peptides from our library and enumeration from each of the resultant random samples what percentage of randomly selected peptides are less stable than expected based on amino acid composition.

(C) Benchmarking of the DegronID algorithm. (Top left). Substrates known to be degraded by KLHL15, marked in red, score in the top 0.2% of our library for similarity to the GLB1L(2) FRYV motif characterized in our study. (Top right). Distribution of BioPlex 3.0 KLHL15 interacting proteins compared to all human proteins in our library for similarity to the GLB1L(2) FRYV motif. (Bottom right) Boxplot showing that KLHL15 interacting proteins skew towards scoring as similar to the GLB1L(2) FRYV motif. (Bottom left) FR[FY] motif obtained from sequence alignment of KLHL15 interacting proteins, using sequence intervals from each protein that score as most similar to GLB1L(2) by DegronID.

(D) Illustration of ranked degron similarity search based on DegronID score for eight selected degrons with validated cognate E3 either ASB7 (top, red) or KLHL15 (bottom, blue). X axis indicates rank of the 260k peptides in our library, y axis indicates DegronID score for each peptide. Peptides for the eight selected degrons are colored and labelled, with color indicating cognate E3.

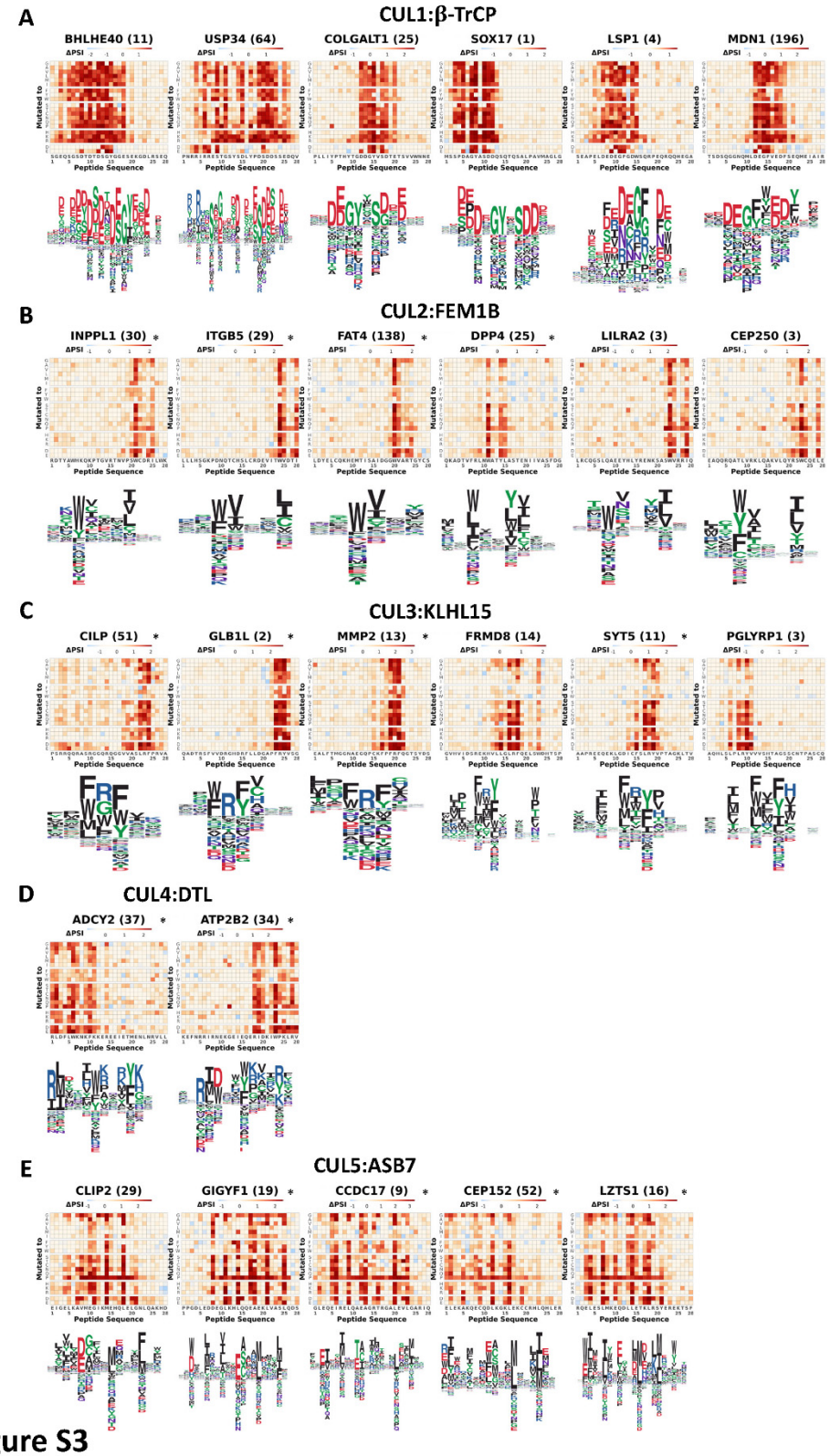
A
CUL1:β-TrCP
BHLHE40 (11)
USP34 (64)
COLGALT1 (25)
SOX17 (1)
LSP1 (4)
MDN1 (196)
B
CUL2:FEM1B
INPPL1 (30) *
ITGB5 (29) *
FAT4 (138) *
DPP4 (25) *
LILRA2 (3)
CEP250 (3)
C
CUL3:KLHL15
CILP (51) *
GLB1L (2) *
MMP2 (13) *
FRMD8 (14)
SYT5 (11) *
PGLYRP1 (3)
D
CUL4:DTL
ADCY2 (37) *
ATP2B2 (34) *
E
CUL5:ASB7
CLIP2 (29)
GIGYF1 (19) *
CCDC17 (9) *
CEP152 (52) *
LZTS1 (16) *
ΔPSI
Mutated to
Peptide Sequence

Figure S3

Figure S3. DegronID predicted peptides with similar degron motifs in the same cluster. Related to Figure 5.

For each meta-cluster indicated in Figure 4, including (A) CUL1:β-TrCP, (B) CUL2:FEM1B, (C) CUL3:KLHL15, (D) CUL4: DTL, (E) CUL5:ASB7, the mutagenesis heatmaps and logo plots of selected peptides with similar motifs were shown. Individual peptides mapped by CRISPR screening, or validated to be the substrates of the corresponding cognate E3 ligase were marked with asterisks.

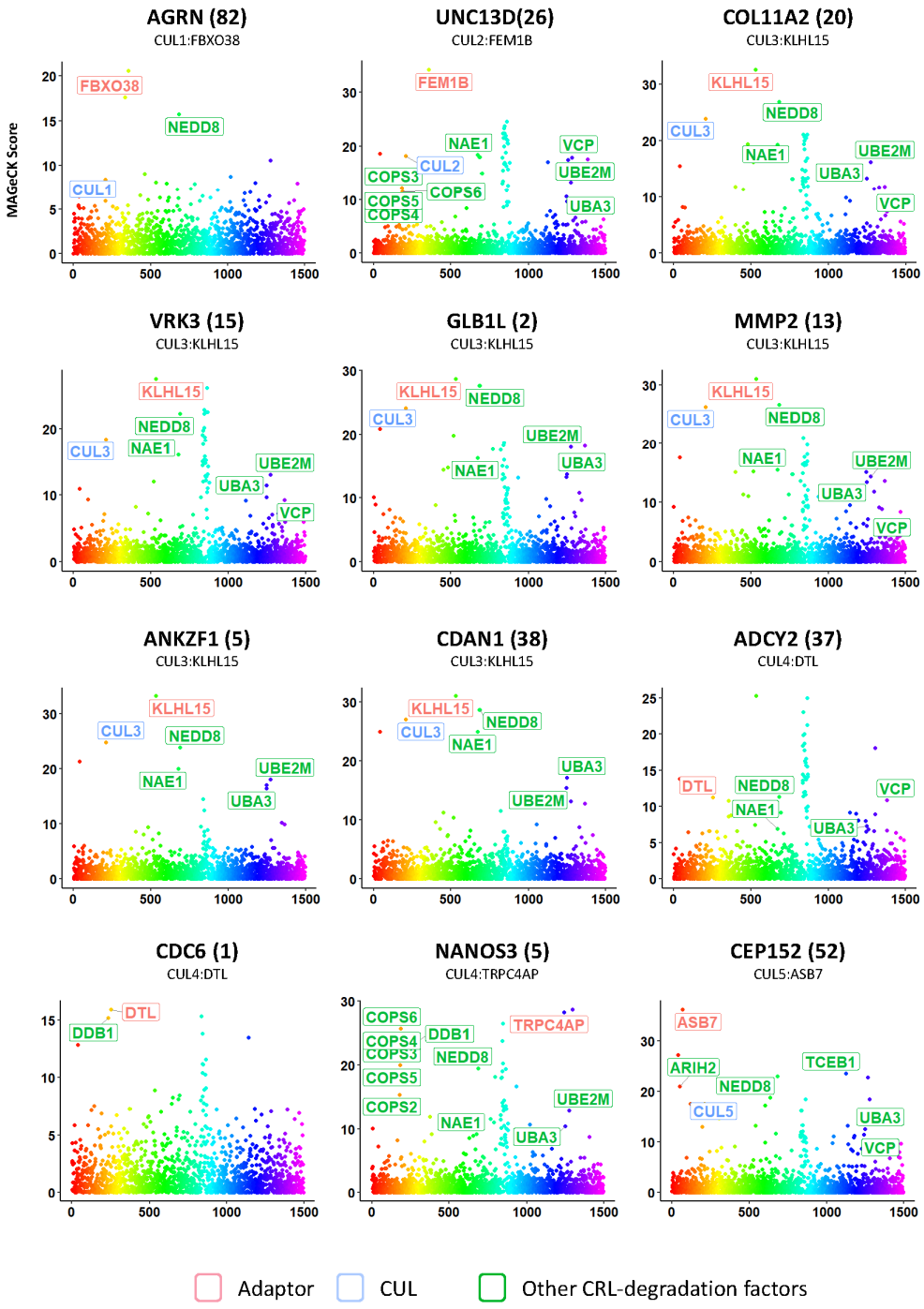
AGRN (82)
CUL1:FBXO38
UNC13D(26)
CUL2:FEM1B
COL11A2 (20)
CUL3:KLHL15
VRK3 (15)
CUL3:KLHL15
GLB1L (2)
CUL3:KLHL15
MMP2 (13)
CUL3:KLHL15
ANKZF1 (5)
CUL3:KLHL15
CDAN1 (38)
CUL3:KLHL15
ADCY2 (37)
CUL4:DTL
CDC6 (1)
CUL4:DTL
NANOS3 (5)
CUL4:TRPC4AP
CEP152 (52)
CUL5:ASB7
MAGeCK Score
Adaptor
CUL
Other CRL-degradation factors

Figure S4

Figure S4. Additional CRISPR screens that identified the cognate E3 ligases for CRL-degron peptides. Related to Figure 6.

For each indicated peptide, CRISPR screening results are shown. For the CRISPR screens, the results were first analyzed by MAGeCK and the significantly enriched Cullin-adaptor pairs were identified and shown (Table S7; see STAR Methods for details).

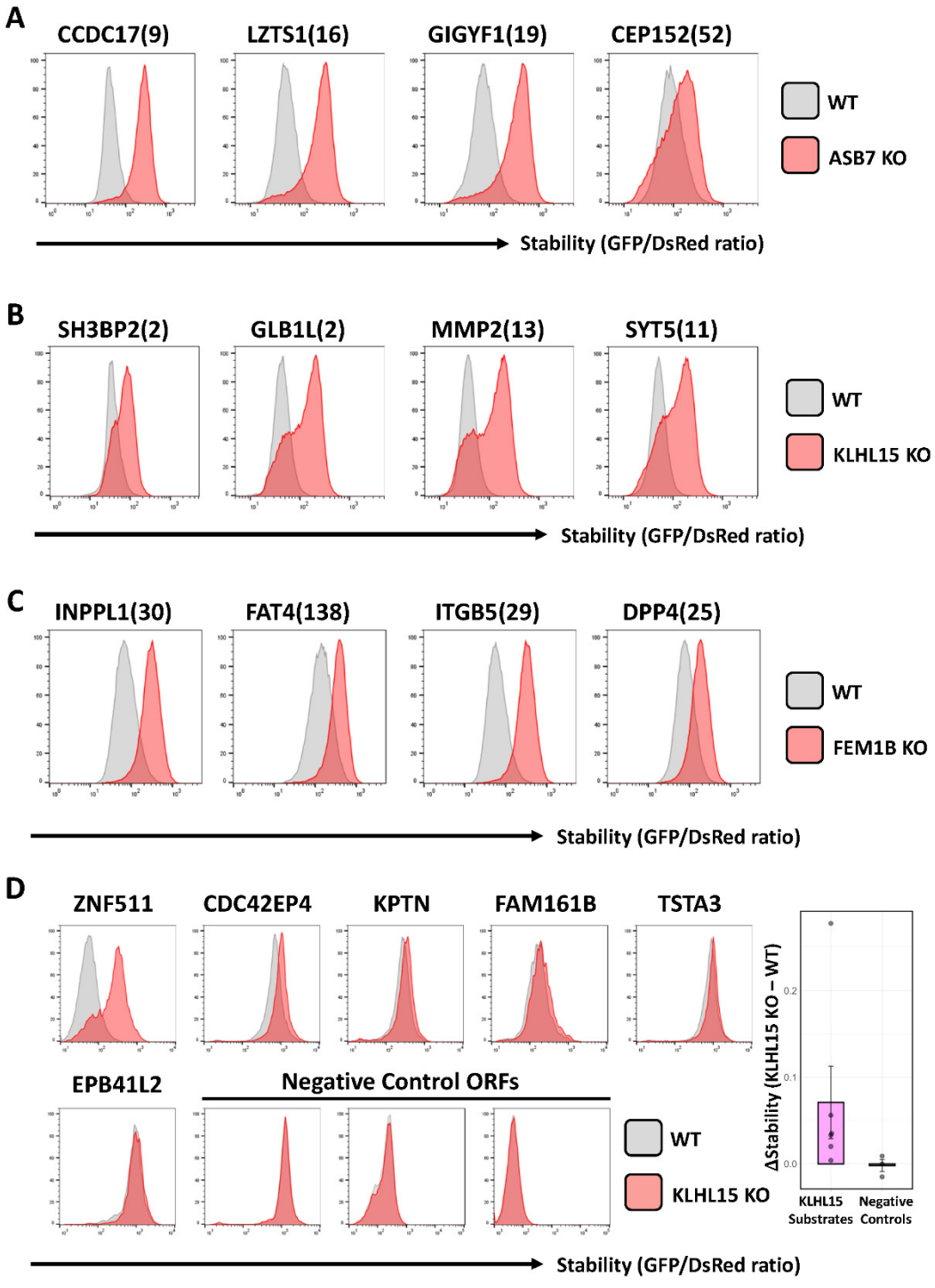
A
CCDC17(9)
LZTS1(16)
GIGYF1(19)
CEP152(52)
WT
ASB7 KO
Stability (GFP/DsRed ratio)
B
SH3BP2(2)
GLB1L(2)
MMP2(13)
SYT5(11)
WT
KLHL15 KO
Stability (GFP/DsRed ratio)
C
INPPL1(30)
FAT4(138)
ITGB5(29)
DPP4(25)
WT
FEM1B KO
Stability (GFP/DsRed ratio)
D
ZNF511
CDC42EP4
KPTN
FAM161B
TSTA3
EPB41L2
Negative Control ORFs
WT
KLHL15 KO
Stability (GFP/DsRed ratio)
ΔStability (KLHL15 KO – WT)
0.2
0.1
0.0
KLHL15 Substrates
Negative Controls

Figure S5

Figure S5. Selected CRL-degron peptides encoding similar motifs were validated as substrates of the same cognate E3 ligase individually. Related to Figure 6.

Peptides encoding motifs resembling that of (A) ASB7; (B) KLHL15; (C) FEM1B were individually validated as the substrate of the E3 ligase by comparing their stabilities in WT and E3 KO condition. The KO was generated by lentiviral infection of an sgRNA targeting the CRL-adaptor, followed by puromycin selection to select the cells expressing the sgRNA. (D) ORFs containing motifs for KLHL15 and identified in BioPlex 3.0 as KLHL15 interacting proteins were individually validated as KLHL15 substrates by comparing their stabilities in WT and KLHL15 KO cells. Three other randomly selected proteins lacking a FRY-like domain or any known association to KLHL15 were also measured as negative controls. In the bar plot to the right, each point represents the change in modal stability between the KLHL15 KO vs. WT cells for one ORF. Putative KLHL15 substrates are gathered on the left column, overlaying the pink bar, and negative control ORFs overlay the grey bay. The bar heights represent the mean of all points in that group. Error bars represent standard error of the mean.

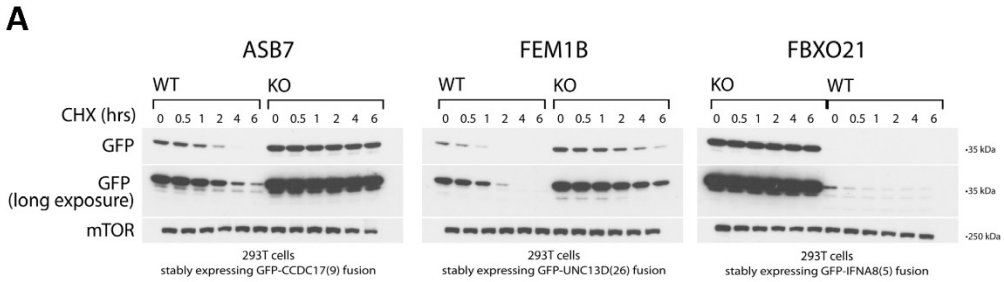

B

```
ASB7:CEP152_52
   1  ELEKAKQECQDLKGKLEKCCRHLQHLER 28
      CCHHHHHHHHHHHHHHHHHHHHHHHCC
      957999999999988999999999969
ASB7:GIGYF1_19
   1  PPGDLEDDEGLKHLQQEAEKLVASLQDS 28
      CCCCCCHHHHHHHHHHHHHHHHHHCCC
      998875799999999999999998589
ASB7:LZTS1_16
   1  RQELESLMKEQDLLETKLRSYEREKTSF 28
      CHHHHHHHHHHHHHHHHHHHHHHHCCC
      848999999888999999888876789
FBXO21:IFNA8_5
   1  TKDSSAALDETLLDEFYIELDQQLNDLE 28
      CCCCHHHHHHHHHHHHHHHHHHHHCCC
      998689999999999999999997799
FBXO38:ZFHX4_40
   1  VSSERSLPEEEWRAVIGDIYQCKLCNYN 28
      CCCCCCCCHHHHHHHHCCCEEEEEEECC
      988888868999998689665568867 9
```

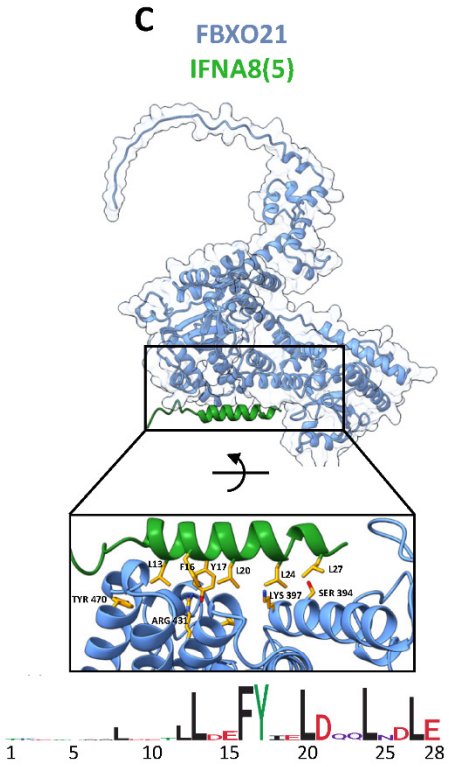

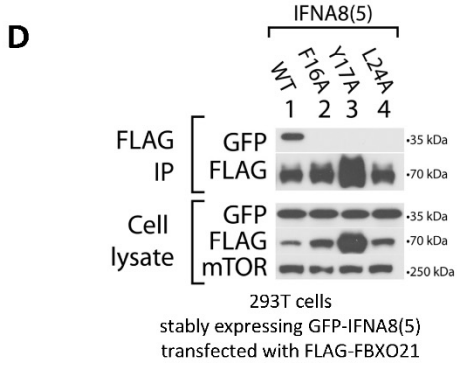

Figure S6

Figure S6. Half-life assay, peptides regulated by FBXO38, FBXO21 and ASB7 are predicted to encode alpha-helical structures by secondary structure prediction program PROTEUS2. Related to Figure 7.

(A) Cycloheximide chase immunoblot for FBXO21:IFNA8(5), ASB7:CCDC17(9), and FEM1B:UNC13D(26).

(B) Alpha-helical structure predictions are shown for the indicated peptides.

(C) Docking structure for FBXO21:IFNA8(5) as predicted by AlphaFold2. Sidechains of critical degron residues mapped by saturation mutagenesis are shown and labelled with single-letter amino acid codes. Sidechains of potential degron-interacting FBXO21 residues are shown and labelled with three-letter amino acid codes.

(D) Co-immunoprecipitation immunoblot data for FBXO21 KO 293T cells stably expressing IFNA8(5) (WT or mutant) fused to GFP and transfected with Flag-FBXO21.

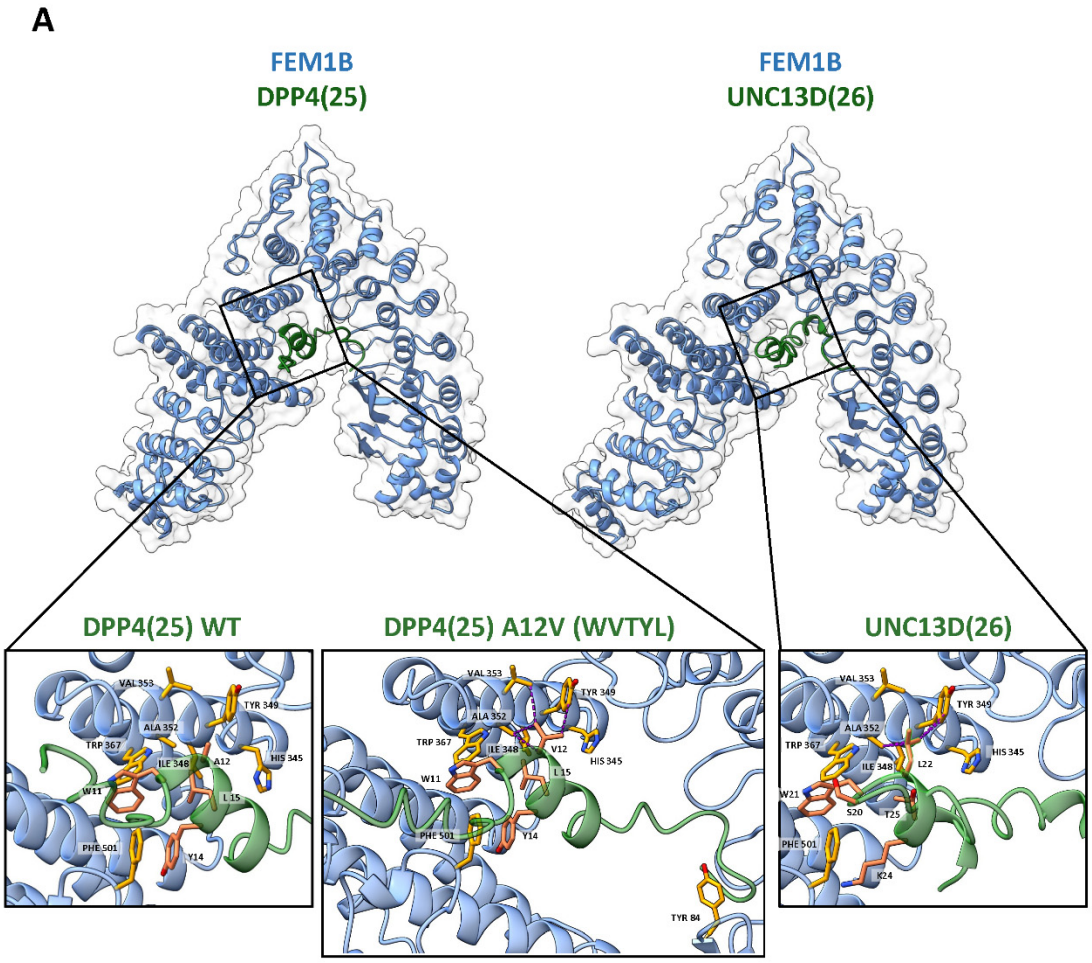
A
FEM1B
DPP4(25)
FEM1B
UNC13D(26)
DPP4(25) WT
DPP4(25) A12V (WVTYL)
UNC13D(26)
VAL 353
TYR 349
ALA 352
TRP 367
ILE 348
A12
HIS 345
W11
L 15
PHE 501
Y14
V12
TYR 84
L22
W21
S20
T25
K24

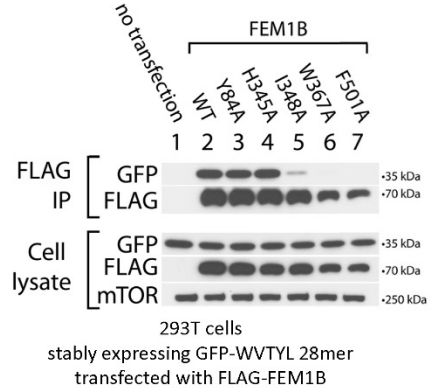
B
no transfection
FEM1B
WT
Y84A
H345A
I348A
W367A
F501A
1 2 3 4 5 6 7
FLAG IP
GFP
FLAG
Cell lysate
GFP
FLAG
mTOR
35 kDa
70 kDa
250 kDa
293T cells
stably expressing GFP-WVTYL 28mer
transfected with FLAG-FEM1B

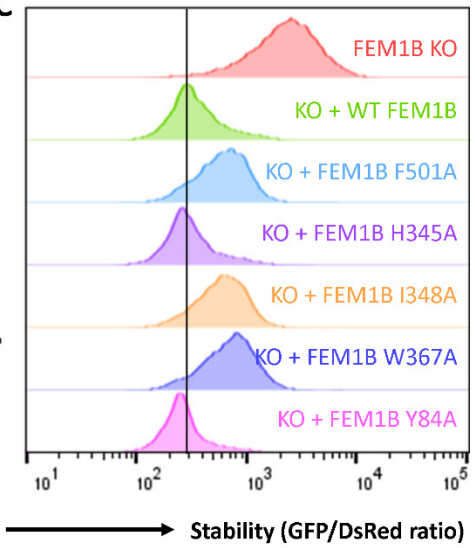
C
FEM1B KO
KO + WT FEM1B
KO + FEM1B F501A
KO + FEM1B H345A
KO + FEM1B I348A
KO + FEM1B W367A
KO + FEM1B Y84A
10^1
10^2
10^3
10^4
10^5
Stability (GFP/DsRed ratio)

Figure S7

Figure S7. E3-degron docking by AlphaFold2 identified critical degron residues consistent with that revealed by saturation mutagenesis, co-immunoprecipitation, and GPS. Related to Figure 7.

(A) Docking structures for FEM1B to identified degron peptides from DPP4(25) and UNC13D(26). In the zoomed-in windows, candidate critical residues on both the ligase and degron are highlighted. For DPP4(25), docking for WT peptide (…WATYL…) and optimized mutant peptide (…WVTYL…) are shown. Shown degron residues are labelled with single-letter amino acid codes. Sidechains of FEM1B residues that were mutagenized in validation experiments are shown and labelled with three-letter amino acid codes. Purple dashed lines indicate atomic contacts made by FEM1B with DPP4(25) A12, WVTYL 28mer V12, or UNC13D(26) L22. Contacts were identified through ChimeraX as intermolecular pairs of atoms with VDW overlap > -0.4Å, which produced similar results to using atomic center-center distance < 4.0Å.

(B) Co-immunoprecipitation immunoblot data for FEM1B KO 293T cells stably expressing an optimized FEM1B degron peptide (…WVTYL…) fused to GFP and transfected with Flag-FEM1B (WT or mutant).

(C) Flow stability data for GFP-optimized FEM1B degron peptide (…WVTYL…) with KO, stably expressed WT or stably expressed mutant FEM1B. The residues Y84 and H345 do not touch the degron and their mutations show WT stability and continue to bind the degron peptide as expected.